



저작자표시-비영리-변경금지 2.0 대한민국

이용자는 아래의 조건을 따르는 경우에 한하여 자유롭게

- 이 저작물을 복제, 배포, 전송, 전시, 공연 및 방송할 수 있습니다.

다음과 같은 조건을 따라야 합니다:



저작자표시. 귀하는 원저작자를 표시하여야 합니다.



비영리. 귀하는 이 저작물을 영리 목적으로 이용할 수 없습니다.



변경금지. 귀하는 이 저작물을 개작, 변형 또는 가공할 수 없습니다.

- 귀하는, 이 저작물의 재이용이나 배포의 경우, 이 저작물에 적용된 이용허락조건을 명확하게 나타내어야 합니다.
- 저작권자로부터 별도의 허가를 받으면 이러한 조건들은 적용되지 않습니다.

저작권법에 따른 이용자의 권리는 위의 내용에 의하여 영향을 받지 않습니다.

이것은 [이용허락규약\(Legal Code\)](#)을 이해하기 쉽게 요약한 것입니다.

[Disclaimer](#)

**Effects of the Intranuclear Delivery of  
Nuclear Factor Kappa B p65 on Root and  
Bone Regeneration in a Rat Model of Tooth  
Replantation**

**Seunghan Mo**

The Graduate School

Yonsei University

Department of Dentistry

**Effects of the Intranuclear Delivery of  
Nuclear Factor Kappa B p65 on Root and  
Bone Regeneration in a Rat Model of Tooth  
Replantation**

Directed by Professor Hyung-Jun Choi

A Dissertation Thesis

Submitted to the Department of Dentistry  
and the Graduate School of Yonsei University  
in partial fulfillment of the requirements  
for the degree of Doctor of Philosophy in Dental Science

**Seunghan Mo**

August 2021

This certifies that the dissertation of Seunghan Mo is approved.



Thesis Supervisor: Choi, Hyung-Jun



Song, Je Soen



Kang, Chung-Min



Jung, Ui-Won



Shin, Yooseok

The Graduate School

Yonsei University

August 2021

## 감사의 글

부족한 제가 박사과정을 마치고 학위논문이 완성되기까지 많은 분들의 헌신이 있었습니다. 이 글을 통해 감사의 인사를 드리고자 합니다.

제가 소아치과 의사로서 박사로서 성장할 수 있게 많은 보살핌과 가르침을 주신 최형준 교수님 감사합니다. 교실을 떠나서도 교수님께서 주신 온정을 가슴에 품고 따뜻한 소아치과 의사로 살아가고자 합니다. 연구 방향을 제시해 주시고 연구설계와 진행에 많은 도움을 주신 송제선 교수님, 좋은 연구의 기회를 주셔서 감사합니다. 끝까지 논문을 완성할 수 있도록 저를 격려해 주시고 학술지에 출간하는데 많은 도움을 주신 강정민 교수님, 덕분에 논문이 나올 수 있었습니다. 동물실험 및 데이터 정리를 위해 많은 노고를 해주신 전미정 박사님, 감사했습니다. 수십 번 반복된 힘든 동물실험을 불평없이 함께한 후배 배지수, 김성진, Munkhulzii Erdenebulgan 선생님의 헌신에도 미안함과 고마움의 마음을 함께 전합니다. 바쁘신 중에도 시간을 내어 논문 심사와 건설적인 조언을 해주신 정의원 교수님, 신유석 교수님께도 감사의 인사를 드립니다.

늘 한결 같은 모습으로 소아치과 의사로서 귀감을 보여주신 최병재 교수님, 환자에 대한 열정과 헌신을 일깨워 주신 이제호 교수님, 늘 따뜻한 미소로

저희들을 가르쳐 주시던 김성오 교수님. 덕분에 제가 소아치과 의사로 성장할 수 있었습니다. 의국 생활을 함께했던 소아치과 동기들 감사합니다. 좋은 시간도 힘든 시간도 흘러 흘러 소중한 추억으로 남았습니다.

마지막으로 항상 저를 믿고 지켜봐 주신 부모님께 이 논문을 바칩니다. 당신의 헌신과 사랑으로 여기까지 올 수 있었습니다. 늘 나를 믿어주고 힘이 되어 주는 소중한 사람 하림씨에게도 고마움과 사랑을 전하며 이 기쁨을 함께 나누고 싶습니다. 많은 분들의 도움과 헌신을 잊지 않고 남은 인생 환자들에게 사랑을 베풀며 살아가겠습니다. 감사합니다.

2021년 8월

모승한 드림

## Table of Contents

<b>Abstract</b> .....	<b>vii</b>
<b>I. Introduction</b> .....	<b>1</b>
<b>II. Materials and Methods</b> .....	<b>4</b>
1. Production of nucleus-transducible form of p65-TMD (nt-p65-TMD) .....	4
2. In vitro study .....	5
3. In vivo study .....	9
4. Statistical Analyses .....	13
<b>III. Results</b> .....	<b>14</b>
1. Generation and transduction efficiency of nt-p65-TMD .....	14
2. Viability and NO release of nt-p65-TMD-treated RAW264.7 cells .....	14
3. Osteoclast differentiation of nt-p65-TMD-treated RAW264.7 cells .....	16
4. Replantation of rat maxillary first molar .....	19

<b>IV. Discussion</b> .....	<b>20</b>
<b>V. Conclusion</b> .....	<b>30</b>
<b>VI. References</b> .....	<b>31</b>
<b>Abstract (in Korean)</b> .....	<b>39</b>

## List of Tables and Figures

<b>Table 1.</b> qPCR forward and reverse primer sequences. The annealing procedures were performed at 60°C for all primers .....	<b>8</b>
<b>Table 2.</b> Scores for quantitative analysis in micro-computed tomography image.....	<b>11</b>
<b>Table 3.</b> Scores for quantitative analysis in histological examination .....	<b>12</b>
<b>Figure 1.</b> The concept of nt-p65-TMD.....	<b>3</b>
<b>Figure 2.</b> Viability and NO release of nt-p65-TMD-treated RAW264.7 cells.....	<b>16</b>
<b>Figure 3.</b> Osteoclast differentiation of nt-p65-TMD in RAW264.7 cells .....	<b>19</b>
<b>Figure 4.</b> Two-dimensional horizontal microcomputed tomography images of rat maxillary first molars 4 weeks after replantation .....	<b>22</b>
<b>Figure 5.</b> Histological analysis of replanted rat maxillary first molars 4 weeks after replantation.....	<b>25</b>
<b>Figure 6.</b> Differences in the degree of bone resorption, root resorption, inflammation in the PDL, and inflammation at the epithelial insertion between the two groups	<b>26</b>

## **Abstract**

# **Effects of the Intranuclear Delivery of Nuclear Factor Kappa B p65 on Root and Bone Regeneration in a Rat Model of Tooth Replantation**

Seunghan Mo

*Department of Dentistry*

*The Graduate School, Yonsei University*

(Directed by Professor Hyung-Jun Choi)

After avulsion and replantation, extracted tooth has a risk of root and bone resorption. The present study aimed to demonstrate that intra-nuclear transducible form of transcription modulation domain of p65 (nt-p65-TMD) can suppress osteoclast differentiation in vitro, and reduce bone resorption in a rat model of tooth replantation. Cell viability and nitric oxide release were evaluated in RAW264.7

cells using CCK-8 assay and Griess reaction kit. Osteoclast differentiation was evaluated using quantitative reverse transcriptase-polymerase chain reaction (RT-PCR) and tartrate-resistant acid phosphatase (TRAP) staining. Thirty-two maxillary rat molars were extracted and stored in saline (n=10) or 10  $\mu$ M nt-p65-TMD solution (n=22) before replantation. After 4 weeks, specimens were scored according to the inflammatory pattern using micro-computed tomography (CT) imaging and histological analyses. nt-p65-TMD treatment resulted in significant reduction of nitric oxide release and osteoclast differentiation as studied using PCR and TRAP staining. Further, micro-CT analysis revealed significant decrease in bone resorption in the nt-p65-TMD treatment group ( $p < 0.05$ ). Histological analysis of nt-p65-TMD treatment group showed that not only bone and root resorption, but also inflammation of the periodontal ligament and epithelial insertion was significantly reduced ( $p < 0.05$ ). These findings suggest that nt-p65-TMD has the unique capabilities of regulating bone remodeling after tooth replantation.

---

**Keywords:** Nuclear factor kappa B; intra-nucleus delivery; osteoclast; tooth replantation

# **Effects of the Intranuclear Delivery of Nuclear Factor Kappa B p65 on Root and Bone Regeneration in a Rat Model of Tooth Replantation**

Seunghan Mo

*Department of Dentistry*

*The Graduate School, Yonsei University*

(Directed by Professor Hyung-Jun Choi)

## **I. Introduction**

Tooth avulsion is defined as the complete dislocation of tooth from the alveolar socket as a result of trauma, and it is characterized by compromised neurovascular supply, pulp necrosis, and loss of periodontal ligament (PDL) cells (Panzarini, et al., 2008). Tooth replantation is an acceptable option post avulsion to preserve the structures adherent to the root surface. The greatest concerns in tooth replantation are preservation of PDL vitality, cementum integrity, and minimal bacterial contamination (Trope, et al., 1995; Selvig, et al.,

1992). The outcome of periodontal healing depends on several factors, including extra-alveolar period, storage medium, damage of PDL cells, root development, and pulp condition (Andreasen, et al., 2008).

In order to minimize the adverse effects of avulsion, root surface treatments have been investigated for their ability to preserve PDL cell vitality (Panzarini, et al., 2008; Pearson, et al., 2003). In cases of delayed tooth replantation, necrotic remnants of PDL cells stimulate the development of external root resorption, which may lead to early tooth loss (Andreasen, et al., 2008; Souza, et al., 2018). Several substances, such as sodium fluoride, stannous fluoride, tetracycline, citric acid, calcium hydroxide, bisphosphonates, have been used to treat the root surface of avulsed teeth to increase their retention rate (Poi, et al., 2013). Root resorption is enhanced by substances released from inflammatory cells in the surrounding tissues, such as osteoclast activating factor, macrophage chemotactic factor, and prostaglandins rate (Gunraj, 1999). Considering the root resorption characteristics, the regulation of transcription factors related to inflammatory response is an effective strategy to control inflammation-related bone and root resorption after replantation.

Nuclear factor kappa B (NF- $\kappa$ B) is a key mediator for both physiological immunity and pathological inflammation. NF- $\kappa$ B controls gene expression of inflammatory mediators, such as cytokines, chemokines, and major histocompatibility complex proteins, and has immune regulation-associated function (Ghosh, et al., 1999). Interestingly, inhibition of NF- $\kappa$ B p65 (RelA) subunit suppresses inflammation and modulates immune function; specific blockade of p65 was found to reduce osteoclastogenesis and increase bone

formation (Alles, et al., 1999). Previously, nucleus-transducible form of p65-transcription modulation domain (TMD), named nt-p65-TMD, conjugated with an Hph1-protein transduction domain (PTD) was developed that could translocate efficiently into the nucleus and interfere with p65 transcription by targeting the promoters of p65-target genes (Park, et al., 2015; Cheon, et al., 2017; Cheon, et al., 2018). Nt stands for nuclear transduction, and is the part that enables intranuclear protein delivery without a receptor. TMD refers to a transcriptional regulatory domain that competitively interferes with transcriptional activity in the promoter of the target gene p65 (Figure 1).

This study aimed to investigate the effect of interactomic inhibition of endogenous p65 on the secretion of inflammatory cytokines and osteoclast differentiation after tooth replantation. In the present study, I examined the role of nt-p65-TMD in cellular cytotoxicity and osteoclast differentiation in vitro. In addition, I investigated the therapeutic effects of nt-p65-TMD on inflammation-related bone and root resorption after tooth replantation in a rat model.

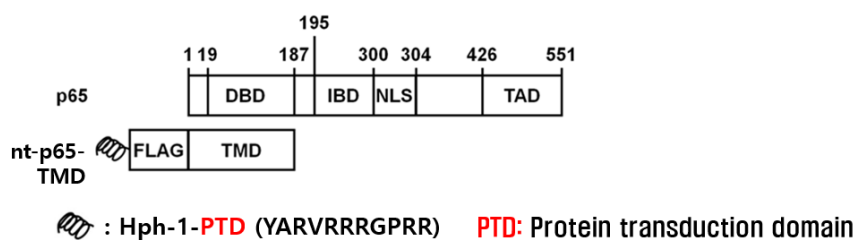


**Figure 1.** The concept of nt-p65-TMD.

## II. Materials and Methods

### 1. Production of nucleus-transducible form of p65-TMD

To generate DNA construct of nt-p65-TMD, DNA sequences encoding the N-terminus of p65 (a.a 1-187) and Hph-1-PTD were amplified by PCR and inserted into the pET-28a (+) vector (Novagen Merck Millipore, Billerica, MA, USA). The DNA construct was transformed into *Escherichia coli* BL21 CodonPlus (DE3)-RIPL strain (Invitrogen, Carlsbad, CA, USA), and protein expression was induced for 5 h at 37 °C with 1 mM isopropyl- $\beta$ -D-thiogalactopyranoside (GenDEPOT, Barker, TX, USA). After sonicating the harvested cells in lysis buffer (10 mM imidazole, 50 mM NaH<sub>2</sub>PO<sub>4</sub>, 300 mM NaCl, pH 8.0), soluble fraction of the lysates was separated by centrifugation (12,000 rpm for 10 min at 4 °C). The soluble proteins were loaded to HisTrap HP chromatography column (GE Healthcare Life Sciences, Marlborough, MA, USA) using Acta pure (GE Healthcare Life Sciences), and protein-bound chromatography column was washed with wash buffer (40 mM imidazole, 50 mM NaH<sub>2</sub>PO<sub>4</sub>, 300 mM NaCl, pH 8.0). Proteins were eluted with elution buffer (500 mM imidazole, 50 mM NaH<sub>2</sub>PO<sub>4</sub>, 300 mM NaCl, pH 8.0). The eluted proteins were loaded into HiTrap SP HP chromatography column in ion-exchange chromatography binding buffer (50 mM NaH<sub>2</sub>PO<sub>4</sub>, pH 6.0) using Acta pure. Bound proteins were washed with SP wash buffer (50 mM NaH<sub>2</sub>PO<sub>4</sub>, 300 mM NaCl, pH 6.0),

and then target proteins were eluted with SP elution buffer (50 mM NaH<sub>2</sub>PO<sub>4</sub>, 1 M NaCl, pH 7.0). The buffer containing eluted proteins was exchanged into 10% glycerol PBS using PD-10 Sephadex G25 (GE Healthcare Life Sciences).

## **2. In vitro study**

### **2.1. Cell culture and cell viability**

RAW264.7 cells were obtained from the Korean Cell Line Bank and cultured in Dulbecco's Modified Eagle Medium (DMEM; Invitrogen) containing 10% fetal bovine serum (FBS; Invitrogen), 100 U/mL penicillin, 100 µg/mL streptomycin (Invitrogen), and 0.2% amphotericin B (Invitrogen) at 37 °C in 5% CO<sub>2</sub>. To evaluate the cell viability, RAW264.7 cells were plated at a concentration of 25,000 cells/well in a 24-well plate. After 24 h, cells were treated with nt-p65-TMD or LY294002 for 2 h. After 24 h, the quantity of water-soluble colored formazan from the Cell Counting Kit (CCK)-8 assay (Dojindo Laboratories, Kumamoto, Japan) formed by the activity of dehydrogenases in living cells was measured using a spectrophotometer (Benchmark Plus microplate spectrophotometer, Bio-Rad Laboratories Inc., Hercules, CA, USA) at 450 nm. In this study, LY294002 was used as a positive inhibitor of NF-κB. There are various inhibitors that inhibit the activity of NF-κB, one of which is LY294002. At this time, LY294002 acts as a PI3K inhibitor. PI3K is an upper transcription factor of NF-κB, and it has been shown that inhibition of PI3K activity inhibits the activity of NF-κB (Avni, et al., 2012; Kim, et

al., 2005). Cell viability assay data were obtained from three independent experiments, with all samples run in triplicate.

## **2.2. Western blot**

After nt-p65-TMD treatment in a dose-dependent manner for 2 h, RAW264.7 cells were lysed and the cell lysate was electrophoresed and transferred onto polyvinylidene difluoride (PVDF) membranes (Bio-Rad Laboratories Inc.). The membrane was blocked using blocking buffer (4% bovine serum albumin in Tris-buffered saline containing Tween 20 (TBST)) to prevent non-specific binding of antibodies. Blocked membrane was incubated with anti-DYKDDDDK (FLAG) or anti- $\beta$ -actin antibody (Cell signaling, Beverly, MA, USA) at 4 °C overnight. After TBST wash, anti-mouse IgG or anti-rabbit IgG (Abcam, Cambridge, UK) was used to detect each primary antibody. For the chemiluminescence reaction, ECL reagent (Bio-Rad Laboratories Inc.) was added onto the membrane and the signal was observed using ChemiDoc (Bio-Rad Laboratories Inc.).

## **2.3. Nitric oxide (NO) assay**

RAW264.7 cells were seeded into 24-well plates at a density of  $2.5 \times 10^4$  cells/well. After nt-p65-TMD or LY294002 treatment in dose-dependent manner for 2 h, the cells were incubated with LPS (0.1  $\mu\text{g}/\text{mL}$ ) for 20 h at 37 °C in CO<sub>2</sub> incubator. To determine the nitrite release in the culture media, presumed to reflect the NO levels, Griess reaction was used, wherein 100  $\mu\text{L}$  cell culture medium was mixed with 100  $\mu\text{L}$  Griess reagent (Invitrogen)

and incubated at room temperature for 30 min. The NO concentration was determined at 540 nm using a spectrophotometer (Bio-Rad Laboratories Inc.)

#### **2.4. Osteoclast differentiation**

RAW264.7 cells were seeded onto 24-well plates at a density of  $1 \times 10^4$  cells/well and treated with nt-p65-TMD or LY294002 for 2 h; DMEM was replaced with Minimum Essential Medium (MEM) alpha (Invitrogen) containing 10% FBS and 10 ng/mL of receptor activator of nuclear factor- $\kappa$ B ligand (RANKL) (PeproTech Inc., Rocky Hill, NJ, USA), and the cells were incubated for 3 days at 37 °C in CO<sub>2</sub> incubator. Tartrate-resistant acid phosphatase (TRAP) staining was performed using TRAP/ALP staining kit (WAKO, Osaka, Japan). Total RNA was isolated using RNeasy Mini Kit (Qiagen, Valencia, CA, USA) according to manufacturer's instructions. Integrity and concentration of the extracted RNA was evaluated using a spectrophotometer (NanoDrop ND-2000, Thermo Scientific, Waltham, MA, USA). Next, 500 ng RNA aliquots were reverse transcribed to cDNA using a Maxime RT premix kit [oligo d(T)15 primer; Intron Biotechnology, Seongnam, Gyeonggi, Korea] according to manufacturer's instructions. A quantitative real-time PCR (qPCR) assay was performed with SYBR Premix Ex Taq (Takara Bio Inc., Otsu, Japan) and a real-time PCR system (ABI 7300, Applied Biosystems, Carlsbad, CA, USA) as per manufacturer's instructions. The qPCR conditions were 95 °C for 10 sec followed by 40 cycles of 95 °C for 5 sec and 60 °C for 30 sec, with a final 5-min extension at 72 °C. Expression for each gene was normalized to that of glyceraldehyde-3-phosphate

dehydrogenase (GAPDH), and the relative expression levels of the target genes were calculated using the  $2^{-\Delta\Delta C_t}$  method (Livak and Schmittgen, 2001). The specific primers for each gene are listed in Table 1.

**Table 1.** qPCR forward and reverse primer sequences. The annealing procedures were performed at 60°C for all primers.

Gene	Forward Primer sequence (5'–3')	Reverse Primer sequence (5'–3')
CTSK	GGGATGTTGGCGATGCA	CCAGCTACTTGAGGTCCATCTTC
NFATc1	CACTGGCGCTGCAACAAGA	CATTCCGGAGCTCAGCAGAATA A
TRAF6	ACCTGAACGCGCCTTCTG	CATCCAGCTGACTCGTTTCATAA
TRAP	CAAAGGTGCAGCCTTTGTGTC	TCACAGTCCGGATTGAGCTCA
GAPDH	CTGGCACAGGGTATACAGGGT TAG	ACTGGTGCCGTTTATGCCTTG

Abbreviations: CTSK, gene encoding cathepsin K; NFATc1, gene encoding nuclear factor of activated T-cells, cytoplasmic 1; TRAF6, gene encoding TNF receptor associated factor 6; TRAP, gene encoding tartrate-resistant acid phosphatase; GAPDH, gene encoding glyceraldehyde-3-phosphate dehydrogenase.

### **3. In vivo study**

#### **3.1. Replantation of rat maxillary first molar**

The procedure for replantation of rat maxillary first molar was performed in accordance with protocol approved by the Institutional Animal Care and Use Committee of Yonsei University (#2018-0214). nt-p65-TMD, diluted to 10  $\mu$ M in saline, was used for the in vivo study. Thirty-two 6-week male Sprague Dawley rats (Orient Bio, Seoul, Korea) weighing 200–250g were used in this study. 6-week rats are adolescence, which is the period when the apex of the tooth is not completely closed. The number of study samples was determined by considering the significance level through a pilot study. To facilitate the extraction, 0.4%  $\beta$ -aminopropionitrile (Sigma, St. Lois, MO, USA) mixed in distilled water was administered to the rats along with the feed 3 days prior to extraction. The maxillary left right molar was atraumatically extracted under anesthesia with ketamine (0.1 mL/100 g, Yuhan, Seoul, Korea) and xylazine (0.05 mL/100 g, Bayer Korea, Seoul, Korea). After performing peritomy using Explorer, the tissue was extracted with minimal trauma from the alveolar socket using tissue forceps. To determine the drug effect on PDL healing, the control and experimental groups were divided, based on the teeth treatment, as follows: In the control group (n=10), the extracted teeth were stored in 50 mL of 0.9% physiological saline (pH 6.0) at 4 °C for 5 min, and cotton soaked with 0.9% physiological saline was applied to the alveolar socket to induce thrombus removal and hemostasis. In the experimental group (n=22), the extracted teeth were stored in 10  $\mu$ M nt-p65-TMD solution

(pH 7.22) at 4 °C for 5 min, and cotton soaked with 10  $\mu$ M nt-p65-TMD solution was applied to the alveolar socket. Immediately after the root surface treatment, the teeth were replanted in the original sockets. After replantation, all animals received a single intramuscular dose of 20,000 UI penicillin G benzathine (Tokyo Chemical Industry Co. Ltd., Tokyo, Japan). Animals in both groups were sacrificed under ketamine anesthesia 4 weeks after replantation. The maxilla was removed, washed with saline, and fixed in 10% formalin.

### **3.2. Micro-computed tomography (CT) image analysis**

The extracted maxilla was scanned at 10  $\mu$ m intervals using a micro-CT system (Quantum FX micro-CT, Parkin Elmer, Norwalk, CT, USA), and the tooth images were reconstructed using a software (TRI-3D, Ratoc System Engineering Co., Ltd., Tokyo, Japan). The pixel size was 2.5  $\mu$ m, and the shooting conditions were 0 kV, 200  $\mu$ A, and the rotation angle of 15 minutes was maintained at 180 degrees. As mesiobuccal (MB) root is the largest and allows clear observation of changes, it was selected. A longitudinal image of the replanted tooth was obtained through long axis of the MB root in the mesiodistal direction. In the longitudinal image, the following events were investigated: A. Bone resorption (The extension of bone surface resorption area in contact with the root was measured.); B. Root resorption; C. Ankylosis (direct fusion of bone to root); D. Pulp mineralization. To quantify the changes in bone and root resorption, scores were attributed to the different events listed below (Table 2). The criteria defined in the study for scoring

in micro-CT image analysis and histological examination were in accordance with those described by Poi (Poi, et al., 2018).

**Table 2.** Scores for quantitative analysis in micro-computed tomography image

Event	Score	Characteristics
Bone resorption	0	no resorption present
	1	resorption occurred in <1/3 of the bone surface
	2	resorption occurred in >1/3 and <2/3 of the bone surface
	3	resorption occurred in >2/3 of the bone surface
Root resorption	0	no resorption present
	1	resorption occurred in <1/3 of the root surface
	2	resorption occurred in >1/3 and <2/3 of the root surface
	3	resorption occurred in >2/3 of the root surface
Ankylosis	0	no ankylosis present
	1	ankylosis present
Pulp mineralization	0	no pulp mineralization present
	1	pulp mineralization present

### **3.3. Histological examination**

After the micro-CT scan, the maxilla was decalcified with 10% ethylenediaminetetraacetic acid (pH 7.4; Fisher Scientific Co., Houston, TX, USA) for 3 weeks at room temperature. The degree of decalcification was confirmed by radiographical analysis. After cryotomy, 20–25- $\mu$ m thick section of maxillary first molar was cut from the sagittal plane to the apical axis, and tissues well connected with the apical and apical roots were selected, stained with hematoxylin and eosin, and observed using an optical microscope (Axio Lab, Zeiss, Germany). The degree of inflammatory resorption of the roots, degree of substitutional substitution, PDL status, and degree of inflammation were observed for each group using an optical microscope. For quantitative analysis, in the same as the micro-CT image analysis, only Mesio Buccal root was observed. In the longitudinal section, the following events were investigated: A. Bone resorption; B. Root resorption; C. Inflammation at the epithelial insertion; D. Inflammation in the PDL (Table 3).

**Table 3.** Scores for quantitative analysis in histological examination.

Event	Score	Characteristics
Bone resorption	0	no resorption present
	1	resorption occurred in <1/3 of the bone surface
	2	resorption occurred in >1/3 and <2/3 of the bone surface
	3	resorption occurred in >2/3 of the bone surface
Root resorption	0	no resorption present
	1	resorption occurred in <1/3 of the root surface
	2	resorption occurred in >1/3 and <2/3 of the root surface
	3	resorption occurred in >2/3 of the root surface
Inflammation at the epithelial insertion	0	absence or occasional presence of inflammatory cells
	1	inflammatory process restricted to lamina propria of the internal part of epithelium
	2	inflammatory process extending apically to the small portion of the connective tissue underlying the lamina propria of the internal portion of the gingival epithelium
	3	inflammatory process reaching the proximity of the alveolar bone crest
Inflammation in the PDL	0	absence or occasional presence of inflammatory cells
	1	inflammatory process presents only in the apical, coronal or small lateral area of PDL
	2	inflammatory process reaching more than half of the lateral PDL of the root
	3	inflammatory process in the whole PDL

#### **4. Statistical Analyses**

Statistical analysis was performed with SPSS (version 25.0, SPSS Inc., Chicago, IL, USA). All in vitro experiments were performed at least in triplicate. The normality of the in vitro data was evaluated using the Shapiro-Wilk test ( $p < 0.05$ ). Multiple comparison testing was conducted using the ANOVA ( $p < 0.05$ ), followed by the t-test for comparing control and experimental group ( $p < 0.05$ ). The normality of in vivo study data was evaluated using the Shapiro-Wilk test ( $p < 0.05$ ). Mann Whitney U test ( $p < 0.05$ ) for comparing saline and nt-p65-TMD group was performed with SPSS.

### **III. Results**

#### **1. Generation and transduction efficiency of nt-p65-TMD**

The N-terminal of p65 has TMD comprising DNA-binding amino acid residues and isotype-specific sequences that may play key roles in the functional specificity of p65. To modulate p65-mediated NF- $\kappa$ B functions, I generated transducible fusion protein (p65-TMD) of p65 with Hph-1-PTD (YARVRRRGPRR). nt-p65 was designed as a novel therapeutic to deliver p65-TMD efficiently into the nucleus of the cells *in vitro* and *in vivo*. Thus, the delivered nt-p65-TMD competitively interferes with the transcriptional activity of endogenous p65 at the promoter of p65-target genes (Figure 2A). To examine the intracellular transduction efficiency, I treated RAW264.7 cells with nt-p65-TMD. nt-p65-TMD was effectively transduced into the cells in a dose-dependent manner (Figure 2B) after 2 h treatment.

## 2. Viability and NO release of nt-p65-TMD-treated RAW264.7 cells

Cell viability was evaluated using LY294002 treatment group as positive control. Cells were treated with different concentrations of nt-p65-TMD for 24 h, and cell viability was assessed using CCK-8 assay kit. Cell viability differed significantly for the 2 and 5  $\mu\text{M}$  nt-p65-TMD treatment groups compared to the control group (Figure 2C).

To measure NO release, cells were incubated in the presence of different concentration of nt-p65-TMD and 0.1  $\mu\text{g}/\text{mL}$  LPS for 20 h. Then, the culture supernatant was analyzed for NO. NO release differed significantly at 0.5, 1, and 2 between the nt-p65-TMD treatment and LPS treatment groups (100% of LPS treatment group, Figure 2D).

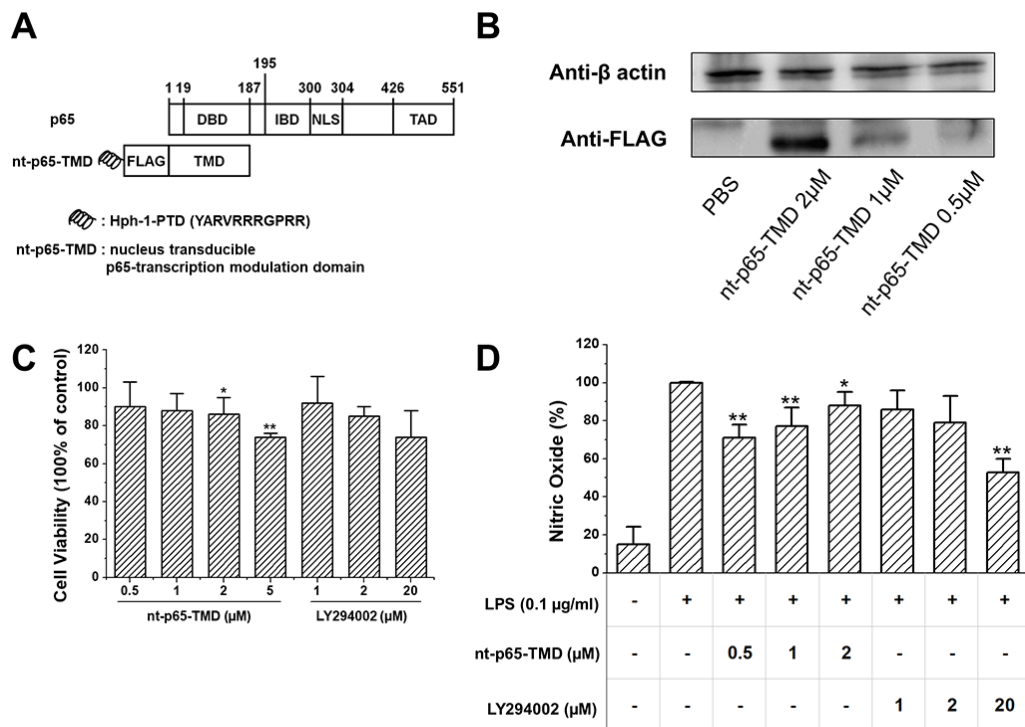


**Figure 2.** (A) Structure of nt-p65-TMD. (B) Transduction efficiency of nt-p65-TMD. Dose-dependent intracellular transduction efficiency of nt-p65-TMD into RAW264.7 cells. nt-p65-TMD was detected by immunoblot analysis with anti-FLAG antibody.  $\beta$ -actin was used as loading control. (C) Cell viability of nt-p65-TMD in RAW264.7 cells. Data show mean  $\pm$  standard deviation values of three independent experiments. \* $p < 0.05$  and \*\* $p < 0.01$  indicate significant differences compared to the control value (100%). (D) NO release of nt-p65-TMD in RAW264.7 cells. Data show mean  $\pm$  standard deviation values of three independent experiments. \* $p < 0.05$  and \*\* $p < 0.01$  indicate significant differences compared to LPS-stimulation value (100%).

### 3. Osteoclast differentiation of nt-p65-TMD-treated RAW264.7 cells

TRAP/ALP staining of RANKL-treated RAW264.7 cells resulted in red-stained osteoclasts. TRAP staining of nt-p65-TMD in RAW264.7 cells. Cells were pretreated with different concentration of nt-p65-TMD for 2 h followed by treatment with 10 ng/mL RANKL for 3 days. Subsequently, RAW264.7 cells were fixed and stained to detect TRAP. The osteoclasts were stained red. nt-p65-TMD treatment group showed lighter TRAP staining than the RANKL treatment group; moreover, higher the nt-p65-TMD concentration, lower was the TRAP staining intensity observed (Figure 3A-F).

The expression of several osteoclast differentiation related genes was confirmed using qPCR. Cells were pretreated with different concentrations of nt-p65-TMD for 2 h followed by treatment with 10 ng/mL RANKL for 3 days. RNA was isolated from RAW264.7 cells and cDNA was synthesized. Expression of tartrate-resistant acid phosphatase (TRAP), TNF receptor associated factor 6 (TRAF6), CathepsinK (CTCK), and nuclear factor of activated T cell, cytoplasmic 1 (NFATc1) was evaluated using quantitative RT-PCR relative to RANKL treatment group (normalized to 100%). Data were obtained from five separate experiments, with all samples run in duplicate. The expression of the genes differed significantly (Figure 3G-J). TRAP, tumor necrosis factor receptor (TNFR)-associated factors (TRAF)6, Cathepsin K (CTSK), and nuclear factor of activated T cell, cytoplasmic 1 (NFATc1) expression was lower in nt-p65-TMD treatment group, and differed significantly compared to that in the RANKL treatment group (Figure 3G-J).

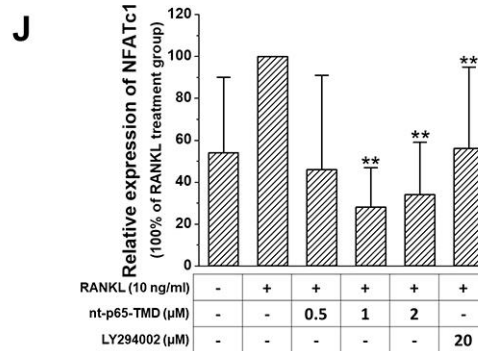
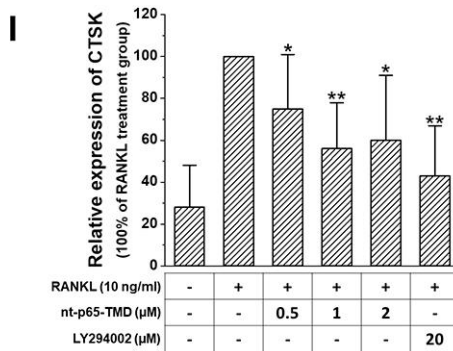
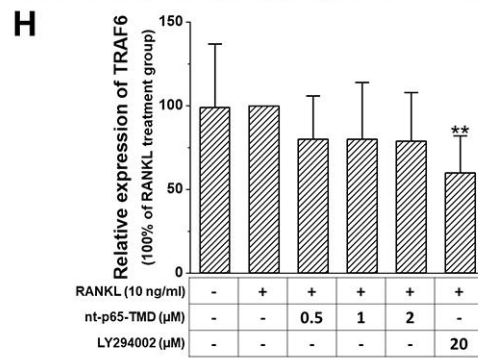
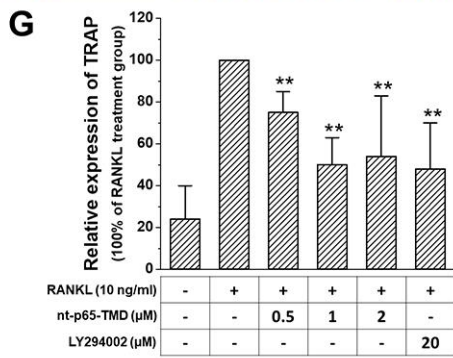
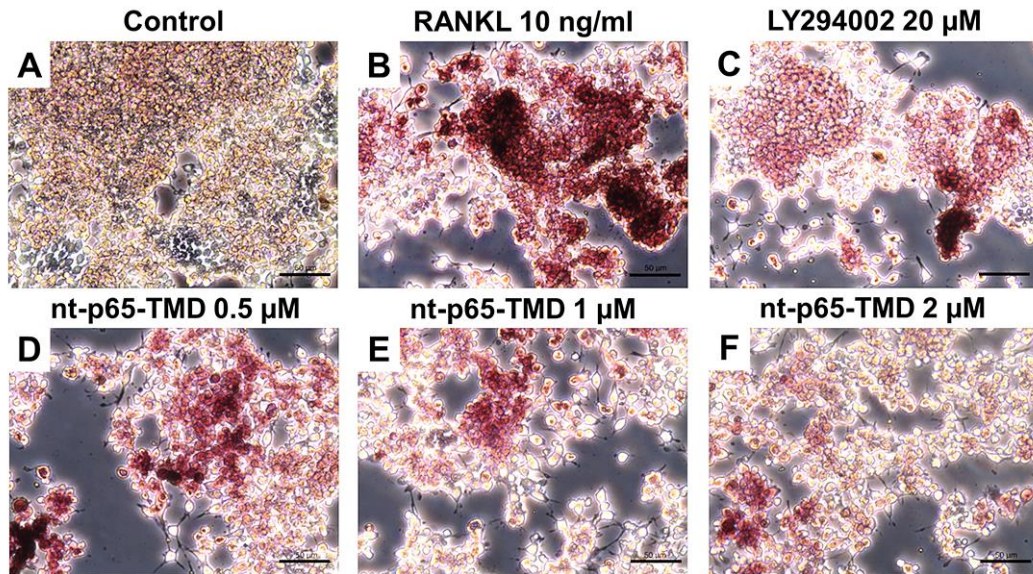


**Figure 3.** Osteoclast differentiation of nt-p65-TMD in RAW264.7 cells (A–F). Scale bars = 50  $\mu$ m. (G–J) Changes in the expression of the osteoclast-related genes of nt-p65-TMD in RAW264.7 cells. The data are expressed as mean  $\pm$  standard deviation values. The expression of the genes differed significantly; t-test and Mann–Whitney U test, \* $p < 0.05$ , \*\* $p < 0.01$

## 4. Replantation of rat maxillary first molar

### 4.1. Radiographic analysis

Radiographic analysis revealed an extensive (score 3) inflammatory absorption of alveolar bone (mean score=2.4) in saline group. Root absorption was further progressed to entire absorption of cementum and dentin (score 3) in five cases of ten (mean score=2.5). In nt-p65-TMD group, bone resorption showed relatively small level of resorption with overall absorption (average=1.68). Root resorption was mild or limited to the surface in most cases (average=1.86). Although cellular cementum destruction occurred in most cases of both the groups, differences in the degree of inflammatory alveolar bone and root resorption between the groups were observed. Localized inflammatory root resorption and alveolar bone resorption occurred in most cases (Figure 4C, F). In the saline group, root and bone resorption occurred more extensively, and resorption to dentin beyond the surface absorption of cementum was observed in several cases (Figure 4B, E). Bone resorption between the groups differed significantly ( $p<0.05$ ), whereas the difference in root resorption was not statistically significant (Figure 4G, H). Further, the difference in replacement resorption was not statistically significant between the saline (mean=0.30) and nt-p65-TMD (mean=0.18) groups (Figure 4I). Similarly, no statistical difference was observed in the degree of pulp mineralization between the saline (mean=0.40) and nt-p65-TMD (mean=0.38) groups (Figure 4J).

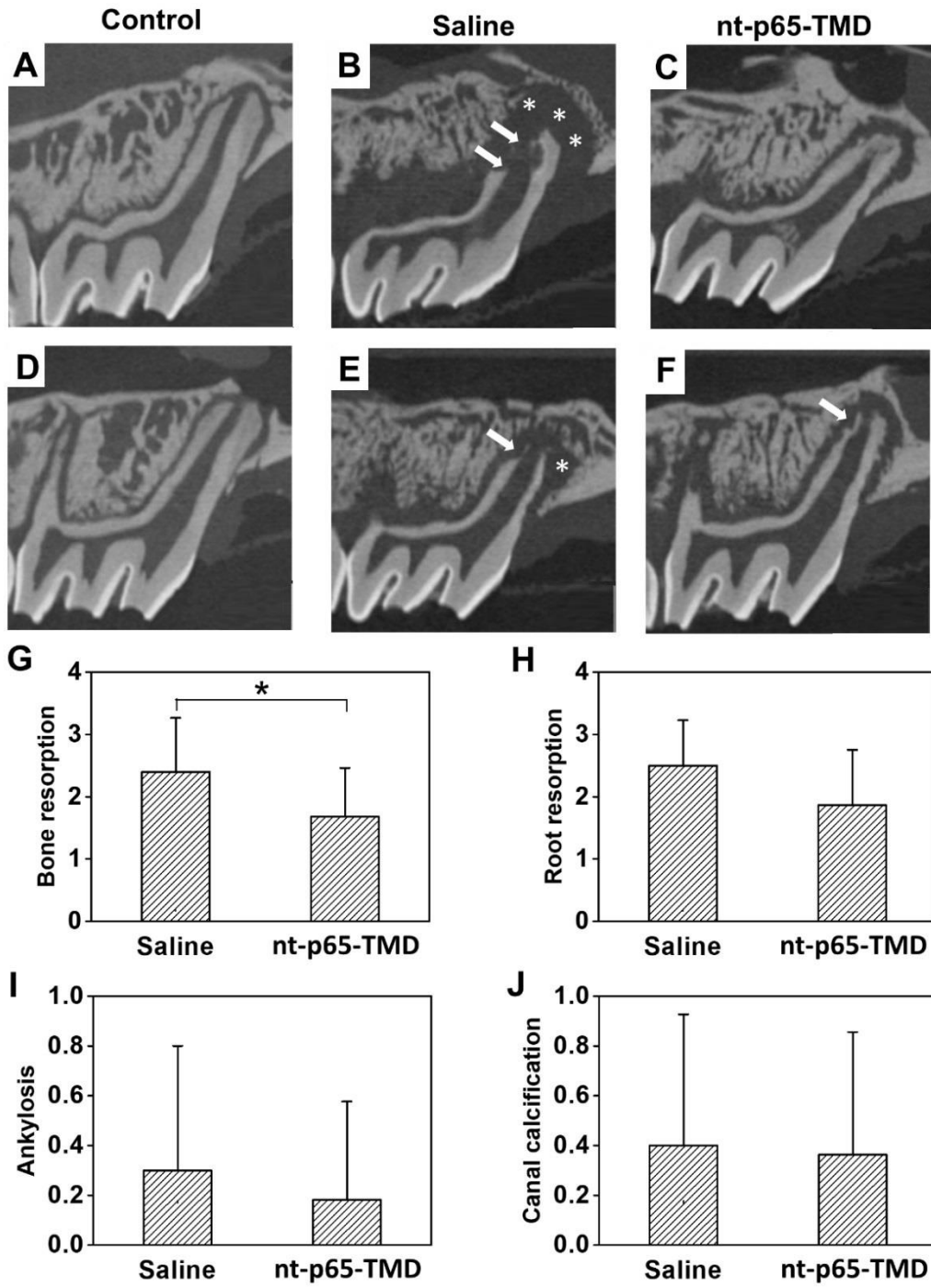


**Figure 4.** Two-dimensional horizontal microcomputed tomography images of rat maxillary first molars 4 weeks after replantation (A, D). Control: The teeth without extraction and replantation. Both bone and root resorption were not observed (B, E). Saline group: 0.9% physiological saline was applied to the extracted teeth surface and alveolar socket. Severe, extensive bone (white asterisk) and root resorption (arrow) were observed (C, F). nt-p65-TMD group: 10  $\mu$ M nt-p65-TMD solution was applied to the surface of the extracted teeth and alveolar socket. A relatively short range of bone resorption (white asterisk) was observed compared to that in the saline group (G–J). Evaluated scores, represented as mean  $\pm$  standard deviation, for (G) bone resorption, (H) root resorption, (I) ankylosis, and (J) pulp mineralization in the saline and nt-p65-TMD groups. Based on the scores of the four categories, only bone resorption showed a significant decrease in the nt-p65-TMD group; Mann–Whitney U test, \* $p$ <0.05.

## 4.2. Histological analysis

The teeth without extraction and replantation were the control group, and Inflammatory root resorption and bone resorption were not observed (Figure 5A, D). Histological analysis revealed a capsular layer of inflammatory cells and fibrous tissues that suppressed the adhesion of PDLs in the saline group. In some cases, resorption was severely progressed, and PDLs and fibroblasts were rarely observed; inflammatory cells, including a large number of lymphocytes, plasma cells, and neutral multinuclear cells, were observed; whereas the apical third was completely lost (Figure 5B, E). Early signs of periodontal tissue regeneration such as periodontal ligament cell proliferation or the appearance of new blood vessels were also not observed. In the nt-p65-TMD group, the PDL space was expanded due to partial alveolar bone resorption, but adhesion of the fibers was relatively good, and the arrangement of PDLs and fibroblasts was partially recovered (Figure 5C, F). Compared to the saline group, the alveolar bone is more mature, the proliferation of periodontal ligament cells is clear, and almost adherence to the root surface is observed. In the apical region and the upper part, the formation of new osteogenic tissue from the existing bone tissue is observed (Figure 5F). Moreover, differences in the degree of alveolar bone resorption, root resorption, inflammation in the PDL, and inflammation at the epithelial insertion were statistically significant ( $p < 0.01$ ) between the two groups (Figure 6G–J). Pulp inflammation was evaluated as related indicators such as inflammatory cells (polymorphonuclear leukocyte, lymphocyte, plasma cell, macrophage, giant cell), cell necrosis, and fibrosis. In both groups, there were no significant changes.

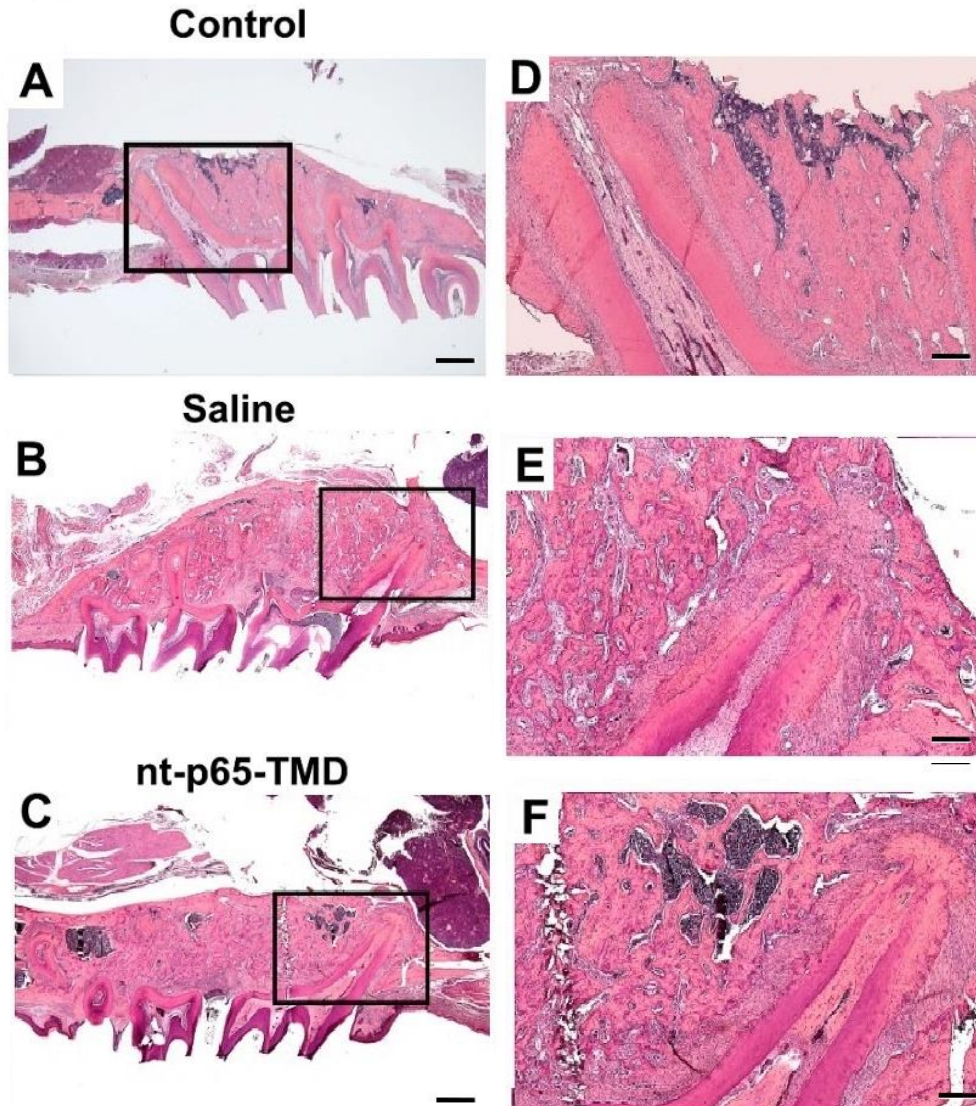


**Figure 5.** Histological analysis of replanted rat maxillary first molars 4 weeks after replantation (A, D). Control group: The teeth without extraction and replantation. (B, E). Saline group: A large number of inflammatory cells were observed, and the apical third was lost by severe inflammatory root resorption (C, F). Hematoxylin-eosin staining, Scale bars = 1mm (applies to A–C) and 500  $\mu$ m (applies to D–F)

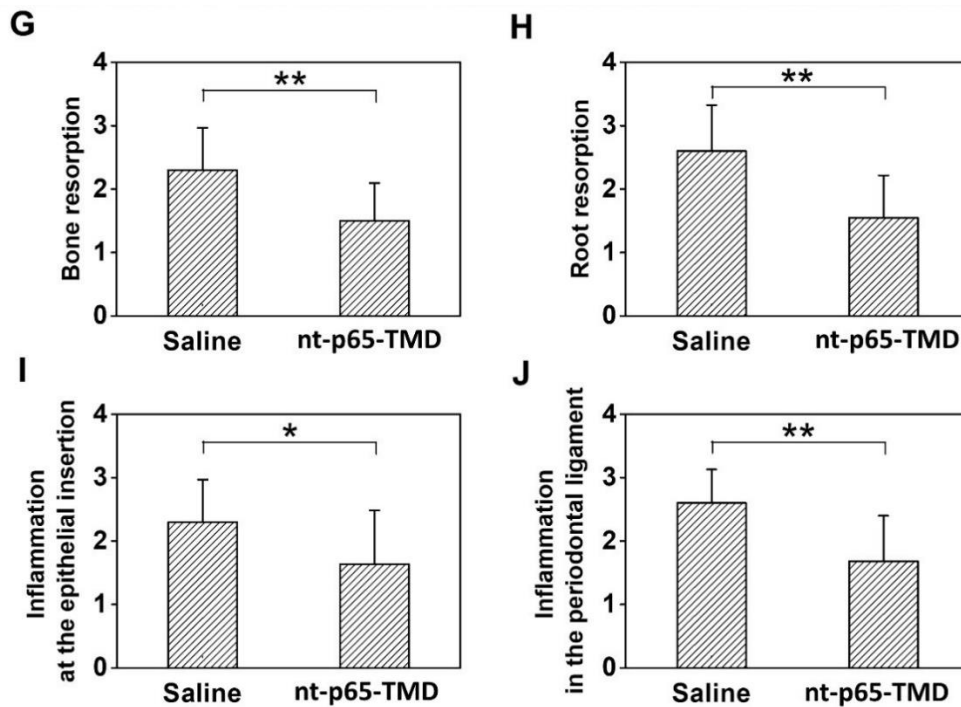


**Figure 6.** nt-p65-TMD group: Localized root resorption and partial recovery of periodontal ligament and fibroblasts were observed (G–J) Evaluated scored, expressed as mean  $\pm$  standard deviation, for (G) bone resorption, (H) root resorption, (I) inflammation at the epithelial insertion, and (J) inflammation in the periodontal ligament in the saline and nt-p65-TMD groups.; Mann–Whitney U test, \* $p < 0.05$ , \*\* $p < 0.01$  (applies to G–J).

## IV. Discussion

In this study, I confirmed a novel therapeutic strategy to suppress inflammation and osteoclastogenesis by intranuclear delivery of the TMD of p65 in vitro and in vivo. nt-p65-TMD, a fusion protein between TMD of p65 and a human origin Hph-1-PTD, could be delivered effectively into the nucleus without influencing the cell viability. nt-p65-TMD significantly reduced osteoclast differentiation and inflammatory response after replantation.

nt-p65-TMD was previously reported to be effective in reducing inflammation. nt-p65-TMD-mediated NF- $\kappa$ B inhibition was reported to have an inhibitory effect on severe sepsis and inflammasome after surgery (Park, et al., 2015; Cheon, et al., 2018). NF- $\kappa$ B is a transcription factor that play an important role in the inflammatory response, and nt-p65-TMD affects the inflammatory response via inhibition of NF- $\kappa$ B activity. Exposure to bacterial products, such as LPS, enhances NO production in RAW264.7 cells (Han, et al., 2019; Lin, et al., 2003). In the present study, the production of NO in the nt-p65-TMD group decreased in a dose-dependent manner, which was more effective at lower concentrations of nt-p65-TMD (0.5 and 1  $\mu$ M). However, the inflammatory response did not decrease below 50% in the NO assay; this may be attributed to the fact that inflammation is induced and regulated through several pathways.

Further, nt-p65-TMD reduced osteoclast differentiation by inhibiting NF- $\kappa$ B. RANKL, expressed by osteocytes, is required for the differentiation of osteoclast precursors into

mature osteoclasts (Nakashima, et al., 2011; Teitelbaum, et al., 2003; Xiong, et al., 2011). The released RANKL binds to its receptor RANK, a member of the TNFR superfamily lacking the intrinsic enzymatic activity that is required for activating downstream signaling molecules (Cheng, et al., 2003). Thus, RANK transduces intracellular signals by recruiting adaptor molecules, such as TRAFs, that then activate mitogen activated protein kinases (MAPKs) and NF- $\kappa$ B (Darnay, et al., 1998; Kobayashi, et al., 2001; Wong, et al., 1998). TRAF6 is the major adaptor protein responsible for mediating RANKL-activated signaling cascades. Activated TRAF6 promotes NF- $\kappa$ B activity (Mizukami, et al., 2002). Decreased expression of TRAF6 leads to suppression of NF- $\kappa$ B function. TRAF6-deficient mice showed severe osteopetrosis (Lomaga, et al., 1999; Naito, et al., 1999). Further, RANK signaling finally induces the amplification of NFATc1 and expression of osteoclastic genes (Takayanagi, et al., 2002). Moreover, NFATc1-knockout mice exhibit osteopetrosis and inhibit osteoclastogenesis in vitro and in vivo (Aliprantis, et al., 2008). In the nt-p65-TMD group of the present study, the expression of TRAF6 and NFATc1 decreased even after RANKL treatment. Eventually, nt-p65-TMD inhibited the function of NF- $\kappa$ B, resulting in inhibition of osteoclast differentiation.

In vivo study revealed that nt-p65-TMD can affect tooth replantation via two processes: inflammation modulation and bone remodeling. First, reduced secretion of the pro-inflammatory cytokine might affect the inflammation-related resorption. After tooth avulsion, the dentinal tubules act as entry-points for bacteria and toxins, causing an inflammatory reaction in the PDL and destroy the root and alveolar bone (Andreasen, et

al., 1966). In the saline group of this study, I observed lack of periodontal repair and occurrence of root resorption in many cases after replantation. These histological observations reportedly accompany inflammatory changes in the PDL along with the resorption of cementum and dentin, and inflammation was detected in the granulation tissue in the PDL that includes a large number of lymphocytes, plasma cells, and neutral multinuclear cells (Moazami, et al., 2012; Okamoto, et al., 1995). Conversely, in the nt-p65-TMD group, inflammation was found as a local feature of surface resorption in the cementum. Interestingly, histological analysis of the nt-p65-TMD group revealed the occurrence of partial recovery of PDLs and fibroblasts. This finding was similar to the previous study in which dexamethasone was applied locally to the replanted teeth of rats (Sae-Lim, et al., 1998). The study demonstrated that local dexamethasone application has anti-inflammatory capacity to control the initial inflammatory response and allows recovery by cementoblast.

In vitro study confirmed that nt-p65-TMD treatment (0.5  $\mu$ M) caused significant reduction in NO release (30%) by inhibiting inflammation, thus indicating the involvement of subunit p65 in inflammation around the replanted teeth. Previous studies have reported the relationship between NF- $\kappa$ B and the protein that forms inflammasome, which is related to the inflammatory response activity (Fann, et al., 2018). In human monocytes, NLRP3 induces NF- $\kappa$ B activity via TLR pathway in bacterial inflammation (Kinoshita, et al., 2015). In addition, nt-p65-TMD used in the current study was reported to inhibit the formation of

inflammasome complex as well as expression of related cytokines after surgery (Cheon, et al., 2018). Therefore, nt-p65-TMD was expected to effectively suppress inflammation during tooth replantation in this study.

Next, *in vivo* study confirmed that nt-p65-TMD affects osteoclast differentiation by inhibiting the function of NF- $\kappa$ B. Reducing the osteoclastic activity is another potential approach for post traumatic treatment. Cell damage resulting from trauma stimulates an inflammatory response that results in the osteoclast-mediated external root resorption (Dempster, et al., 1997). Similar to findings, inhibition of bone resorption was observed after topical application of alendronate to the replanted teeth of rats (Komatsu, et al., 2008; Shibata, et al., 2004), suggesting an inhibition of osteoclast function to be the main function of alendronate. As nt-p65-TMD inhibits not only bone resorption but also root resorption, it may also influence the function of odontoclasts. Further studies are needed to investigate how nt-p65 affects the cells around the replanted teeth.

The present study has several limitations. First, I did not confirm whether nt-p65-TMD was well transduced into the tooth surface and alveolar socket after tooth replantation. However, in previous experiments using Hph-1-PTD domain, the proteins were reportedly well transduced to various cells and tissues, particularly through the skin (Choi, et al., 2006). Therefore, nt-p65-TMD might have sufficiently transduced into the tooth and bone structure in the present study. Of course, it may be questionable whether application to the tooth surface for only 5 min can result in long-term effects. However, saline or nt-p65-TMD was applied to the alveolar socket as well as to the extracted tooth surface, which

could be maintained even after replantation. It will be more meaningful to add an experiment for studying the effects over time post-application. The second, long-term effect of nt-p65-TMD treatment on ankylosis and canal calcification was not evaluated. Further follow-up studies should be performed to confirm the practical clinical applications of this study. Third, in order to effectively process nt-p65-TMD, its optimal concentration of the treatment dose needs to be determined through further experimentation. Moreover, it needs to compare favorably with other anti-inflammation-related transcription factor.

## **V. Conclusion**

In conclusion, nt-p65-TMD can be a novel therapeutic to prevent root and bone resorption after tooth replantation. The present study is the first to demonstrate the possibility of intranuclear delivery of synthetic nuclear factor to the tissue in the healing process after tooth replantation. Furthermore, the strategy can be applied for the development of novel therapeutics for bone remodeling issues in dentistry, especially where a specific transcription factor is known to have a key role in the pathogenesis.

## VI. References

- Panzarini, S.R.; Gulinelli, J.L.; Poi, W.R.; Sonoda, C.K.; Pedrini, D.; Brandini, D.A.  
Treatment of root surface in delayed tooth replantation: A review of literature.  
*Dental Traumatology* 2008(24), 277-282.
- Trope, M.; Moshonov, J.; Nissan, R.; Buxt, P.; Yesilsoy, C. Short vs. Long-term calcium hydroxide treatment of established inflammatory root resorption in replanted dog teeth. *Dental Traumatology* 1995(11), 124-128.
- Selvig, K.A.; Bjorvatn, K.; Bogle, G.C.; Wikesjö, U.M.E. Effect of stannous fluoride and tetracycline on periodontal repair after delayed tooth replantation in dogs. *European Journal of Oral Sciences* 1992(100), 200-203.
- Andreasen, J.O.; Borum, M.K.; Jacobsen, H.L.; Andreasen, F.M. Replantation of 400 avulsed permanent incisors. 4. Factors related to periodontal ligament healing. *Endod Dent Traumatol* 1995(11), 76-89.
- Pearson, R.M.; Liewehr, F.R.; West, L.A.; Patton, W.R.; McPherson, J.C.; Runner, R.R.  
Human periodontal ligament cell viability in milk and milk substitutes. *Journal of Endodontics* 2003(29), 184-186.
- Souza, B.D.M.; Dutra, K.L.; Kuntze, M.M.; Bortoluzzi, E.A.; Flores-Mir, C.; Reyes-Carmona, J.; Felipe, W.T.; Porporatti, A.L.; De Luca Canto, G. Incidence of root

resorption after the replantation of avulsed teeth: A meta-analysis. *Journal of Endodontics* 2018(44), 1216-1227.

Poi, W.R.; Sonoda, C.K.; Martins, C.M.; Melo, M.E.; Pellizzer, E.P.; de Mendonça, M.R.; Panzarini, S.R. Storage media for avulsed teeth: A literature review. *Brazilian dental journal* 2013(24), 437-445.

Gunraj, M.N. Dental root resorption. *Oral Surgery, Oral Medicine, Oral Pathology, Oral Radiology, and Endodontology* 1999(88), 647-653.

Ghosh, S.; Hayden, M.S. New regulators of nf-kappab in inflammation. *Nat Rev Immunol* 2008(8), 837-848.

Alles, N.; Soysa, N.S.; Hayashi, J.; Khan, M.; Shimoda, A.; Shimokawa, H.; Ritzeler, O.; Akiyoshi, K.; Aoki, K.; Ohya, K. Suppression of nf-kappab increases bone formation and ameliorates osteopenia in ovariectomized mice. *Endocrinology* 2010(151), 4626-4634.

Park, S.D.; Cheon, S.Y.; Park, T.Y.; Shin, B.Y.; Oh, H.; Ghosh, S.; Koo, B.N.; Lee, S.K. Intranuclear interactomic inhibition of nf-kappab suppresses lps-induced severe sepsis. *Biochem Biophys Res Commun* 2015(464), 711-717.

Cheon, S.Y.; Kim, J.M.; Kam, E.H.; Ho, C.C.; Kim, E.J.; Chung, S.; Jeong, J.H.; Lee, D.D.; Lee, S.W.; Koo, B.N. Cell-penetrating interactomic inhibition of nuclear factor-kappa b in a mouse model of postoperative cognitive dysfunction. *Sci Rep* 2017(7), 13482.

- Cheon, S.Y.; Kim, J.M.; Kim, E.J.; Kim, S.Y.; Kam, E.H.; Ho, C.C.; Lee, S.K.; Koo, B.N.  
Intranuclear delivery of synthetic nuclear factor-kappa b p65 reduces inflammasomes after surgery. *Biochem Pharmacol* 2018(158), 141-152.
- Park, S.D.; Cheon, S.Y.; Park, T.Y.; Shin, B.Y.; Oh, H.; Ghosh, S.; Koo, B.N.; Lee, S.K.  
Intranuclear interactomic inhibition of nf-kb suppresses lps-induced severe sepsis. *Biochem Biophys Res Commun* 2015(464), 711-717.
- Han, B.; Dai, Y.; Wu, H.; Zhang, Y.; Wan, L.; Zhao, J.; Liu, Y.; Xu, S.; Zhou, L. Cimifugin inhibits inflammatory responses of raw264.7 cells induced by lipopolysaccharide. *Medical science monitor : international medical journal of experimental and clinical research* 2019(25), 409-417.
- Lin, H.Y.; Juan, S.H.; Shen, S.C.; Hsu, F.L.; Chen, Y.C. Inhibition of lipopolysaccharide-induced nitric oxide production by flavonoids in raw264.7 macrophages involves heme oxygenase-1. *Biochem Pharmacol* 2003(66), 1821-1832.
- Nakashima, T.; Hayashi, M.; Fukunaga, T.; Kurata, K.; Oh-Hora, M.; Feng, J.Q.; Bonewald, L.F.; Kodama, T.; Wutz, A.; Wagner, E.F. et al. Evidence for osteocyte regulation of bone homeostasis through rankl expression. *Nat Med* 2011(17), 1231-1234.
- Teitelbaum, S.L.; Ross, F.P. Genetic regulation of osteoclast development and function. *Nature reviews. Genetics* 2003(4), 638-649.
- Xiong, J.; Onal, M.; Jilka, R.L.; Weinstein, R.S.; Manolagas, S.C.; O'Brien, C.A. Matrix-embedded cells control osteoclast formation. *Nat Med* 2011(17), 1235-1241.

- Cheng, X.; Kinosaki, M.; Murali, R.; Greene, M.I. The tnf receptor superfamily: Role in immune inflammation and bone formation. *Immunologic research* 2003(27), 287-294.
- Darnay, B.G.; Haridas, V.; Ni, J.; Moore, P.A.; Aggarwal, B.B. Characterization of the intracellular domain of receptor activator of nf-kappab (rank). Interaction with tumor necrosis factor receptor-associated factors and activation of nf-kappab and c-jun n-terminal kinase. *The Journal of biological chemistry* 1998(273), 20551-20555.
- Kobayashi, N.; Kadono, Y.; Naito, A.; Matsumoto, K.; Yamamoto, T.; Tanaka, S.; Inoue, J. Segregation of traf6-mediated signaling pathways clarifies its role in osteoclastogenesis. *The EMBO journal* 2001(20), 1271-1280.
- Wong, B.R.; Josien, R.; Lee, S.Y.; Vologodskaiia, M.; Steinman, R.M.; Choi, Y. The traf family of signal transducers mediates nf-kappab activation by the trance receptor. *The Journal of biological chemistry* 1998(273), 28355-28359.
- Mizukami, J.; Takaesu, G.; Akatsuka, H.; Sakurai, H.; Ninomiya-Tsuji, J.; Matsumoto, K.; Sakurai, N. Receptor activator of nf-kappab ligand (rankl) activates tak1 mitogen-activated protein kinase kinase kinase through a signaling complex containing rank, tab2, and traf6. *Molecular and cellular biology* 2002(22), 992-1000.
- Lomaga, M.A.; Yeh, W.C.; Sarosi, I.; Duncan, G.S.; Furlonger, C.; Ho, A.; Morony, S.; Capparelli, C.; Van, G.; Kaufman, S. et al. Traf6 deficiency results in osteopetrosis

and defective interleukin-1, cd40, and lps signaling. *Genes & development* 1999,(13), 1015-1024.

Naito, A.; Azuma, S.; Tanaka, S.; Miyazaki, T.; Takaki, S.; Takatsu, K.; Nakao, K.; Nakamura, K.; Katsuki, M.; Yamamoto, T. et al. Severe osteopetrosis, defective interleukin-1 signalling and lymph node organogenesis in traf6-deficient mice. *Genes to cells : devoted to molecular & cellular mechanisms* 1999(4), 353-362.

Takayanagi, H.; Kim, S.; Koga, T.; Nishina, H.; Isshiki, M.; Yoshida, H.; Saiura, A.; Isobe, M.; Yokochi, T.; Inoue, J. et al. Induction and activation of the transcription factor nfatc1 (nfat2) integrate rankl signaling in terminal differentiation of osteoclasts. *Developmental cell* 2002(3), 889-901.

Aliprantis, A.O.; Ueki, Y.; Sulyanto, R.; Park, A.; Sigrist, K.S.; Sharma, S.M.; Ostrowski, M.C.; Olsen, B.R.; Glimcher, L.H. Nfatc1 in mice represses osteoprotegerin during osteoclastogenesis and dissociates systemic osteopenia from inflammation in cherubism. *The Journal of clinical investigation* 2008(118), 3775-3789.

Andreasen, J.O.; Hjorting-Hansen, E. Replantation of teeth. I. Radiographic and clinical study of 110 human teeth replanted after accidental loss. *Acta odontologica Scandinavica* 1966(24), 263-286.

Moazami, F.; Mirhadi, H.; Geramizadeh, B.; Sahebi, S. Comparison of soymilk, powdered milk, hank's balanced salt solution and tap water on periodontal ligament cell survival. *Dent Traumatol* 2012(28), 132-135.

- Okamoto, T.; Okamoto, R. Effect of splinting upon healing after immediate replantation of rat upper incisors. Histomorphological study. *Rev Odontol UNESP* 1995(24), 87-97.
- Sae-Lim, V.; Metzger, Z.; Trope, M. Local dexamethasone improves periodontal healing of replanted dogs' teeth. *Endod Dent Traumatol* 1998(14), 232-236.
- Fann, D.Y.; Lim, Y.A.; Cheng, Y.L.; Lok, K.Z.; Chunduri, P.; Baik, S.H.; Drummond, G.R.; Dheen, S.T.; Sobey, C.G.; Jo, D.G. et al. Evidence that nf- $\kappa$ b and mapk signaling promotes nlrp inflammasome activation in neurons following ischemic stroke. *Molecular neurobiology* 2018(55), 1082-1096.
- Kinoshita, T.; Imamura, R.; Kushiyama, H.; Suda, T. Nlrp3 mediates nf- $\kappa$ b activation and cytokine induction in microbially induced and sterile inflammation. *PloS one* 2015(10), e0119179.
- Dempster, D.W.; Moonga, B.S.; Stein, L.S.; Horbert, W.R.; Antakly, T. Glucocorticoids inhibit bone resorption by isolated rat osteoclasts by enhancing apoptosis. *The Journal of endocrinology* 1997(154), 397-406.
- Komatsu, K.; Shimada, A.; Shibata, T.; Shimoda, S.; Oida, S.; Kawasaki, K.; Nifuji, A. Long-term effects of local pretreatment with alendronate on healing of replanted rat teeth. *Journal of periodontal research* 2008(43), 194-200.

- Shibata, T.; Komatsu, K.; Shimada, A.; Shimoda, S.; Oida, S.; Kawasaki, K.; Chiba, M.  
Effects of alendronate on restoration of biomechanical properties of periodontium  
in replanted rat molars. *Journal of periodontal research* 2004(39), 405-414.
- Choi, J.M.; Ahn, M.H.; Chae, W.J.; Jung, Y.G.; Park, J.C.; Song, H.M.; Kim, Y.E.; Shin,  
J.A.; Park, C.S.; Park, J.W. et al. Intranasal delivery of the cytoplasmic domain of  
ctla-4 using a novel protein transduction domain prevents allergic inflammation.  
*Nat Med* 2006(12), 574-579.
- Avni, D.; Glucksam, Y.; Zor, T. The phosphatidylinositol 3-kinase (pi3k) inhibitor  
ly294002 modulates cytokine expression in macrophages via p50 nuclear factor  
kappa b inhibition, in a pi3k-independent mechanism. *Biochemical pharmacology*  
2012(83), 106-114.
- Kim, Y.H.; Choi, K.-H.; Park, J.-W.; Kwon, T.K. Ly294002 inhibits lps-induced no  
production through a inhibition of nf-kb activation: Independent mechanism of  
phosphatidylinositol 3-kinase. *Immunology letters* 2005(99), 45-50.
- Poi, W.R.; Sonoda, C.K.; Amaral, M.F.; Queiroz, A.F.; França, A.B.; Brandini, D.A.  
Histological evaluation of the repair process of replanted rat teeth after storage in  
resveratrol dissolved in dimethyl sulphoxide. *Dent Traumatol* 2018,  
doi:10.1111/edt.12402.

## 국문요약

# 쥐의 치아 재식 모델에서 Nuclear Factor Kappa B p65 의 핵내 전달이 치근흡수와 골흡수에 미치는 영향 분석

연세대학교 대학원 치의학과

모 승 한

지도교수: 최형준

본 연구는 nt-p65-TMD의 전사 조절 도메인의 핵내 형질 도입이 시험관 내에서 파골세포 분화 및 쥐의 치아재식 모델에서 골흡수 및 치근 흡수에 미치는 영향을 연구하였다.

체외 세포 실험을 통해 nt-p65-TMD이 세포독성 및 파골세포 분화에 미치는 영향을 조사하였다. 세포 생존력 및 산화 질소 방출은 CCK-8 분석 및 Griess 반응 키트를 사용하여 RAW264.7 세포에서 평가하였다. 파골세포 분화는 역전사 효소-중합 효소 연쇄 반응(RT-PCR) 및 타르트레이트 내성 산 포스파타제 (TRAP) 염색을 사용하여 평가하였다.

쥐 재식실험 모델에서 nt-p65-TMD가 치아재식 후 염증성 골흡수와 치근 흡수에 미치는 영향을 조사하였다. 실험은 쥐 상악 어금니 32개를 발치하여 식염수(n=10) 또는 10 $\mu$ M nt-p65-TMD 용액(n=22)을 처리한

후 이식하였다. 4 주 후, 미세 컴퓨터 단층 촬영(micro-CT) 영상 및 조직학적 분석을 사용하여 표본에서 염증의 정도를 평가하였다.

PCR 및 TRAP 염색을 사용하여 연구한 체외 세포 실험결과에서 nt-p65-TMD 처리는 산화 질소 방출 및 파골 세포 분화의 유의미한 감소를 보였다. 쥐 재식 실험의 단층 촬영 분석에서 nt-p65-TMD 처리군에서 골흡수가 현저히 감소하였다 ( $p < 0.05$ ). 조직학적 분석에서 nt-p65-TMD 치료군이 골흡수와 치근 흡수 뿐 아니라 치주 인대의 염증도 감소한 것으로 나타났다. 이러한 결과는 nt-p65-TMD가 염증과 골세포의 분화에 관여하여 재식 후 골형성을 조절하는 가능성을 가지고 있음을 시사한다.

결론적으로, nt-p65-TMD는 치아 재식 후 치근과 골의 재흡수를 방지하는 새로운 치료제가 될 수 있다. 이 연구는 치아 재식 후 치유 과정에서 합성 핵 인자의 핵 내 전달 가능성을 입증했다. 이 방법은 특정 전사 인자가 병인에 중요한 역할을 하는 것으로 알려진 치과의 골 재형성 문제에 대한 새로운 치료제 개발에 적용될 수 있다.

---

**핵심되는 말:** Nuclear factor kappa B, 핵내 전달, 파골세포, 치아 재식